We are IntechOpen,
the world's leading publisher of
Open Access books
Built by scientists, for scientists

6,500
Open access books available

176,000
International authors and editors

190M
Downloads

Our authors are among the

154
Countries delivered to

TOP 1%
most cited scientists

12.2%
Contributors from top 500 universities

BOOK CITATION INDEX
CLARIVATE ANALYTICS
INDEXED

WEB OF SCIENCE™

Selection of our books indexed in the Book Citation Index
in Web of Science™ Core Collection (BKCI)

Interested in publishing with us?
Contact book.department@intechopen.com

Chapter

The Microstructure and Mechanical Properties of the Aluminum Alloy (AA 6061 T6) Under the Effect of Friction Stirs Processing

Emad Toma Bane Karash and Mohammad Takey Elias Kassim

Abstract

The following chapter study the friction stir processes (FSP) is used to improve the surface characteristics of the alloy AA6061-T6 on the surface topography, hardness, tension mechanical characteristics, and microstructures of aluminum alloy, the impacts of friction stir process tool travel and rotation speeds were investigated. All friction stir processes (FSW) in this investigation used a cylindrical tool without a pin that had a 20 mm diameter, rotated at different rotating speeds 800, 1000, 1250, and 1600 rpm, and at different travel speeds 32, 63, and 80 mm per minute. The examination of the current study's data and the test results showed that in stir friction processes, hardness rises with cutting depth. The study of the crystal structure showed that the hardness increased by twice as much for two stages as it did for one stage. Additionally, it was observed that as cutting depth increased, the size of the granules representing engineering defects grew smaller. Additionally, in the case of two stages, the ratio of granule size to friction was twice as high as in the case of one step. According to the results, using a single-stage friction stir process increased yield strength by 18% and tensile strength by 9.5%, while using a two-stage friction stir process increased yield strength by 20.4% and tensile strength by 11.5% when compared to metal basis.

Keywords: friction stir processes, aluminum alloy, linear speed, travel speed, hardness, microstructure

1. Introduction

The lightness of aluminum in comparison to other forms of metal is one of its qualities that led to its widespread application in all industrial sectors. Due to its density, which is around one-third that of steel as an engineering material, and the fact that heat-treatable aluminum alloys may provide a high percentage of resistance, aluminum ranks second in importance only to steel as an engineering material. It ranks third among the earth's accessible elements, behind silicon and oxygen, making it one of the most abundant metals in the crust of the planet.

It also happens to be one of the most chemically efficient metals, making up 7.5% to 8.1% of the weight of the earth's surface [1, 2]. The ability of heat-treated aluminum alloys to withstand corrosion by water, salts, and some other substances makes this metal resistant to natural climate variables, which is another significant characteristic in the business. Aluminum's high affinity for the union with oxygen and the development of a thin surface layer are what cause it to have such a good ability to resist corrosion. From its oxide, it is impenetrable (Al_2O_3). The metal is exposed to air, which causes it to develop. Corrosion is halted by it. As a result, it is used to make tanks for the chemical industry, as well as to make colors and use its powder in paint. An additional benefit of aluminum is that it is a non-toxic metal, making it a valuable material. Corrosion is prevented by it. As a result, it is employed in the creation of tanks for the chemical industry as well as the production of colors and paint using its powder. Aluminum is utilized in the creation of containers for storing food and soft drinks since it is a non-toxic metal in addition to having all these other significant qualities [2, 3]. Numerous previous researchers have examined and investigated the friction stir welding processing parameters for improving the mechanical qualities of the welded joint [4–6]. It would be equivalent to claiming that different joint technology alloys are employed in fabrication because fusion welding has melted a lot of them while producing secondary phases due to thermal absences using base materials as a pin device [7]. Due to this, compared to alloys of various compositions, the temperature distribution in nugget zones (NZs) has risen more gradually. The best solution to this issue is to gather rotational and transverse speeds. The tool is therefore essential in FSW [8]. It has been addressed in detail how to fabricate surface composites with different reinforcement combinations, such as AA7075-TiO_2, AA7075-and-TiO_2-SiC, and TiO_2 + SiC, while maintaining consistent tool rotation, tool travel speed, and number of passes. The same is meant to increase hardness. It has been noted that the friction stir treated surface composite had an average hardness that was 4 times more than the parent metal [9, 10].

2. Friction stir process studies

The technique of friction and stir treatment derives from surface engineering technology, which allows localized removal of plumbing flaws by changing or smoothing the microstructure and enhancing the material's mechanical properties. The investigation of the friction stir process (FSP) for aluminum alloys was the subject of a number of studies.

J. M. Salman [11] investigated the impact of two rotational speeds (710 rpm) and three linear speeds (116, 189, and 303 mm/min) on the mechanical characteristics and microstructure of an aluminum-zinc-magnesium-copper alloy. Shock resistance, elongation, a rise in the hardness value, and an increase in the tensile and yield strength were all seen to increase during the process. Observations were made along the original and treated samples' structural details in great detail. A variety of thermal treatments, including fermentation, equation, and hardness by quenching in water, were applied to several samples that shown improved fermentation process parameters. The outcomes also demonstrated an increase in the heat produced during the procedure. The findings also revealed a drop in the linear speed and an increase in the heat produced throughout the operation when the rotational speed was raised.

A friction stir procedure was used to blend SiC particles with an aluminum alloy type (6351) to create molecular composite materials in a work by V. V. Murali Krishna

et al. in 2015 [12]. Using a friction stir process tool with or without a motor, the samples were rotated and lateral accelerated at constant rates. An optical microscope was used to obtain the (SiC) reinforcements and make measurements of the microstructure of the changed surfaces. At the University of Technology Malaysia, the mechanical characteristics were estimated using the tensile test. The study demonstrated that the number of multi-stage runs results in an improvement in the crystal structure of the friction stir process, and the results of the tensile tests showed an increase in the toughness and hardness of the microstructure for one run of the friction stir process of the models, but a decrease in the durability of the models with the increase in runs, which is attributed to the dissolution of solid precipitates.

The effects of the frictional stir process on the structural and mechanical properties of an aluminum casting alloy with a high degree of hardness were studied by Karthikeyan et al. in 2008 [13], using three different feeding rates (10, 12 and 15 mm/min) and two different tool speeds (1400 and 1800 rpm). It was found that increasing the tool speed for a given feed results in an improvement in the mechanical properties. Additionally, the hardness values of the internal structure of the processed materials rise as a result of the machine's increased rotational speed. As evidenced by the data, the internal structure's hardness values become as close as feasible to the internal structural hardness of the primary materials as one moves away from the weld mass's center. The findings of the mechanical properties process also reveal optimal values at a feed rate of (12 mm/min). It was noted that the average crystal size of (350 nm) in models worked using a machine with a horizontal linear speed of (15 mm/min) and a rotational speed of (1400 rpm) in When the average crystal size was 400 nm) for the same feeding speed and rotational speed. The average crystal size in (25) places on the base material (6.2 m), and it was noted that the average crystal size of (350 nm) in models worked using a (1400 rpm).

In terms of the study, Al-Danaf et al., 2010 [14] examined how the frictional stir process affected commercially rolled sheets (AA5083). A rotary tool with a rotating speed of 430 rpm and a transverse feeding rate of 90 mm/min was used to apply friction stir to the models. And that after this process, a 1.6 m-wide fine crystalline microstructure was obtained. It was discovered that a reduction in the crystal size resulted in a noticeably improved level of ductility and a reduction in forming forces. The ductility was determined using the tensile elongation at a temperature of 250°C, at three stress ratios. The frictional stir procedure increased the ductility of the working materials with a coefficient that varied between (2.6–5) when compared to the ductility of the final product, in the same range of stress rates that were examined. The original metal's Vickers hardness test score was (HV 80), however the number at the center of mass was higher and reached roughly (HV 95).

3. Metal property

Aluminum alloy (T6) - 1 (AA606) heat-treated sheets were employed as the foundation metal in this work. **Table 1** show the alloy's chemical makeup, and **Table 2** that can be trusted provided the alloy's mechanical characteristics. According to Table, this alloy is allowed for use with aluminum alloy [15–18].

4. Initialization of friction stir process (FSP)

Aluminum alloy (AA 6061-T6) with a nominal composition in (Wt. %) was the substance used. The dimensions and thickness of the ingot were adjusted on a milling machine to obtain the necessary dimensions (220 * 30 * 3 mm in size), after which it was prepared in a different way (Butt joint configuration) so that the welding line is perpendicular to the rolling direction. This was done to prevent altering the boards' original composition. Using a set rotational speed for the friction tool and a welding linear speed of 800 rpm and 80 mm/min, the friction stir process was performed on a typical vertical milling machine. In both stages, the friction tool is at varying depths of 25, 50, 100, 150, 200, 300, and 400 m. A single pass of the friction tool was made during the first stage of the samples' friction process, and a double pass was made

Element Materials (%)	Nominal chemical composition	Actual chemical composition
Zn	Max. - 0.15	0.108
Si	0.4–0.8	0.415
Fe	Max. - 0.08	0.408
Ga	—	0.011
Cu	0.15–0.4	0.269
Mn	Max. - 0.15	0.063
Mg	0.8–1.2	0.895
Cr	0.04–0.35	0.208
Ni	—	0.013
Ti	Max. - 0.15	0.017
V	—	0.011
Others each	Max. - 0.05	0.005
Others total	Max. - 0.15	0.025
Al	95.8–98.6	97.552

Table 1.
Chemical composition of AA 6061-T6.

Material properties	Nominal value [15]	Actual value
Tensile Yield Strength MPa	276	245
Ultimate Tensile Strength MPa	310	309
% EL	17	16
Modulus of Elasticity Gpa	69.8	68
Hardness, Vickers	107	101.5
Hardness, Brinell	95	93.5

Table 2.
Mechanical properties of AA 6061-T6.

during the second stage on a plate of thickness (3 mm). **Figure 1** depicts the friction model's dimensions and shape.

The friction stirrer is typically made of carbon tool steel (X12M), which has undergone heat treatment to achieve the desired hardness (62.85 HRC), giving it a high degree of durability and resistance to heat and sulfating. The chemical components of the friction stirrer have also been examined in the Department of Standardization and Quality Control in Baghdad; further information is provided in Appendix (B). The friction tool's diameter was concave (mm 10). The friction tool's geometry, as indicated in **Figure 2**, was utilized. The chemical components of the friction stir process tool utilized are described in full in **Table 3**, which was chosen in accordance with **Table 4**.

All friction stir activities in the mechanical workshop are performed on the vertical milling machine. We also created a straightforward fixture out of carbon steel to hold the components while they were being welded together and fixed using the friction technique. In the present study, four rotational speeds (800, 1000, 1250, and 1600 rpm) and three linear speeds (32, 63, and 80 mm/min) were selected from the factors of frictional stir processes, namely the linear speed of the milling machine table and the rotational speed of the friction tool. To complete the friction stir procedure, the tool was turned clockwise (C.W.). Some models of aluminum alloy and the procedure for carrying out the friction stir process are shown in **Figure 3**.

In order to determine how the frictional stir process affects the alloy's properties, frictional stir operations are carried out on the alloy for one stage (one pass) and two stages (double pass) at various depths **Figure 4**.

For both the first stage and the second stage of the models, light microscopy and scanning electron microscopy were used to analyze the microscopic structure of the friction stir process models. Where I exposed the grain boundaries using Keller's reagent (for a duration of 10–20 sec.) at room temperature and for all samples. The friction zone hardness was measured by applying a load of (27 gm.) for (15 s) using an indenter) of a pyramid shape made of diamonds according to the specification (ASTM-E384) [20]. The precise hardness measurements were performed using a Vicker's micro hardness device (Zwick/Roell Z HV). As shown in **Figure 5**, readings are obtained at three sites for each model, one of which is in the center of the frictional
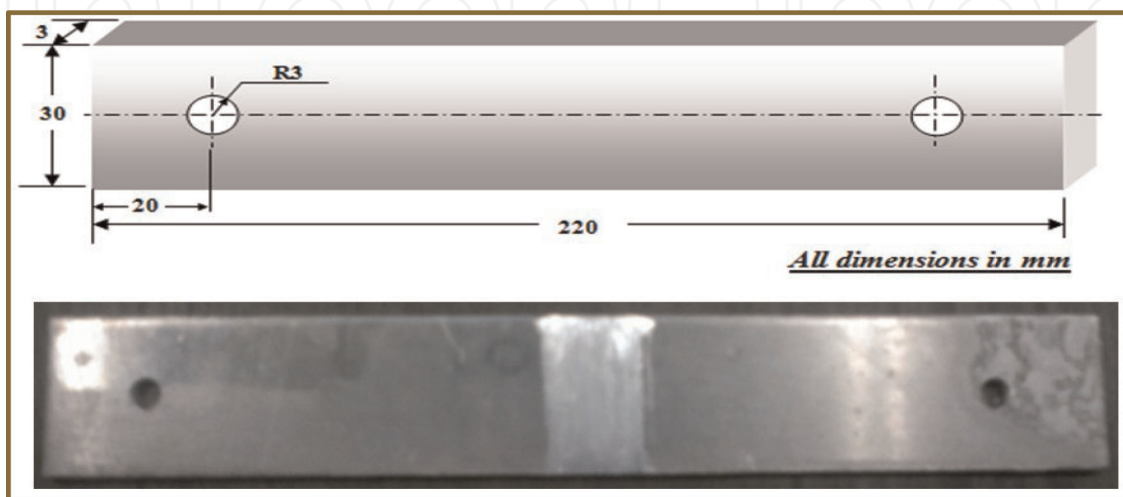

Figure 1.
Displays the size and shape of the alloy friction stir process model (AA6061-T6).
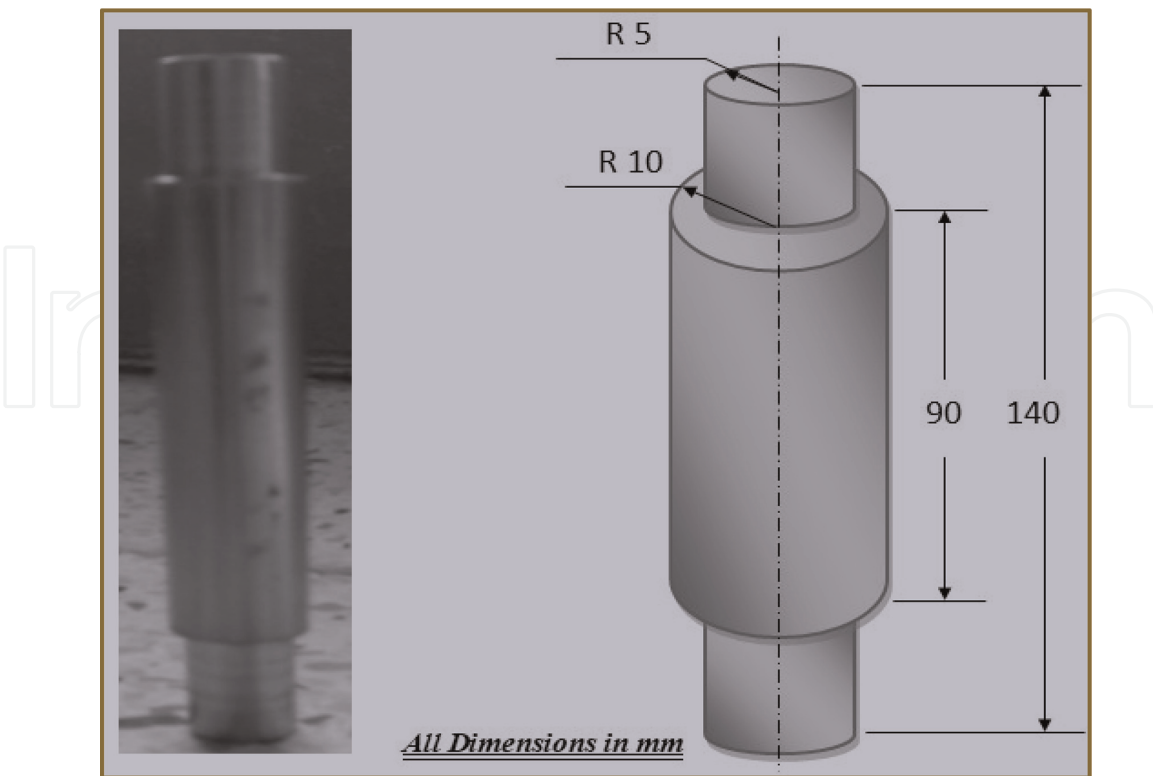
Figure 2.
The tool's geometric design, as used in the friction stir procedure.

Model	Specification	Mechanical tests			
Alloy Steel	ISO 6508	Hardness (HRC)		62.85	
		Chemical composition			
		C %	0.845	Al %	0.007
		Si %	0.265	Co %	0.098
		Mn %	0.240	Cu %	0.118
		P %	0.037	Nb %	0.001
		S %	0.009	Ti %	0.006
		Cr %	4.17	V	1.79
		Mo %	2.31	W	6.52
		Ni %	0.136	Sn %	0.005
		Fe %		Rem.	

Table 3.
Lists the chemical components of the tool used in the friction stir operation.

stir area close to the surface. The other two readings are taken on a straight line to the right and left of the center, with a 1 mm gap between them **Figure 5**. With a rotational speed of 800 rpm and a linear speed of 80 mm/min and different cutting depths (25, 50, 100, 150, 200, 300, 400 m), transverse tensile models for the base metal and friction tool stir process were prepared in two stages, with the first stage being once and the second stage being twice.

	Thickness		
No.	**Alloy**	**mm**	**Tool material**
1	Aluminum alloys	< 12	Tool steel, WC – Co
2	Magnesium alloys	< 6	Tool steel, WC
3	Copper	< 50	Nickel alloys, PCBN (a)
4	Copper alloys	< 11	Tool steel
5	Titanium alloys	< 6	Tungsten alloys
6	Stainless steels	< 6	PCBM, tungsten alloys
7	Low – alloy steels	< 10	WC, PCBN
8	Nickel alloys	< 6	PCBN

a. PCBN, polycrystalline cubic boron nitride

Table 4.
It displays a few of the materials used to make welding tools [19].
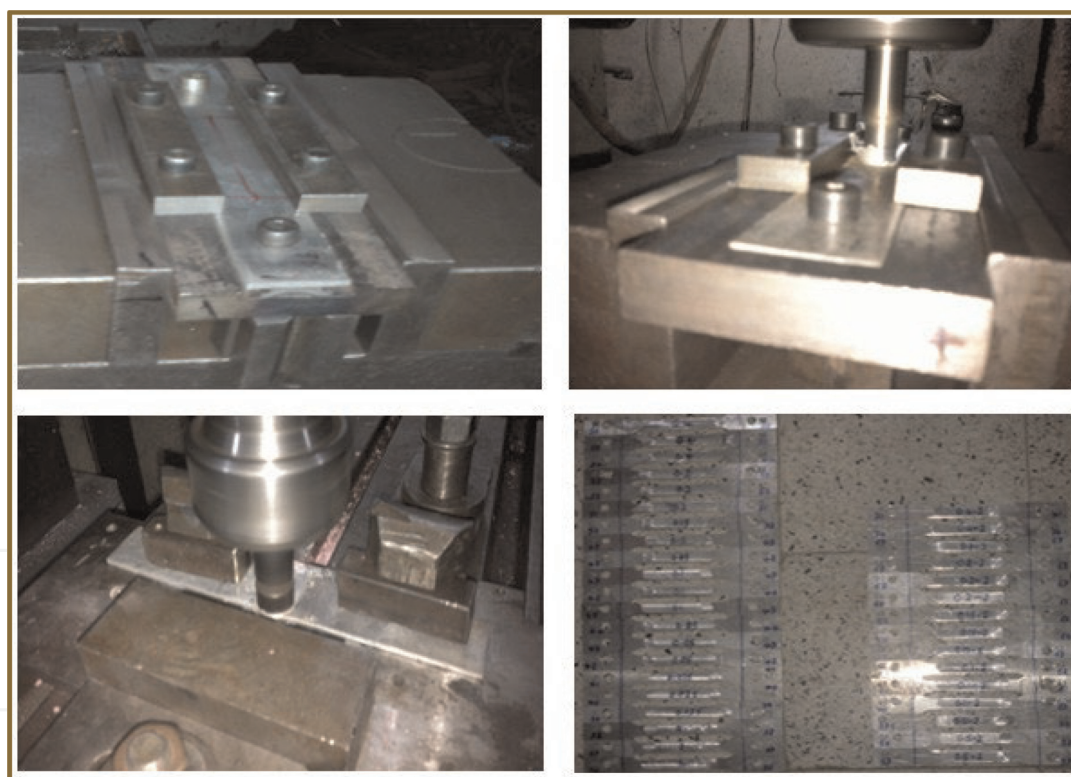
Figure 3.
Frictional stir process of models.

5. Macro and microstructure specimens

Following the friction stir and welding processes, the samples are prepared for microscopic inspection using the following steps:

Samples were created from acrylic material using hot supports after being cut to length and thickness from the cross-section of the area to be investigated. Size and fineness of hydrate (graded from coarse to fine (220, 320, 600, 1000, 1500, 2000 grit). The samples are then polished and polished using diamond paste with a granular
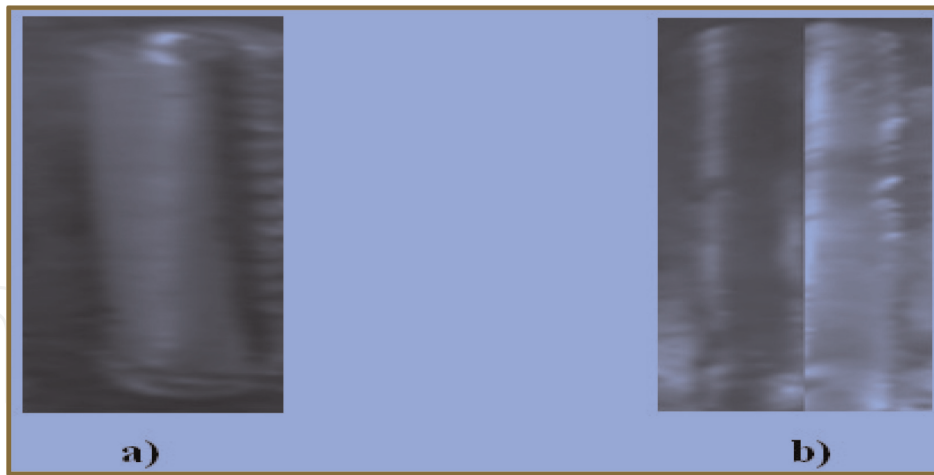
Figure 4.
Multiple stages of friction stir processes for models: A-single stage, b- two stage.
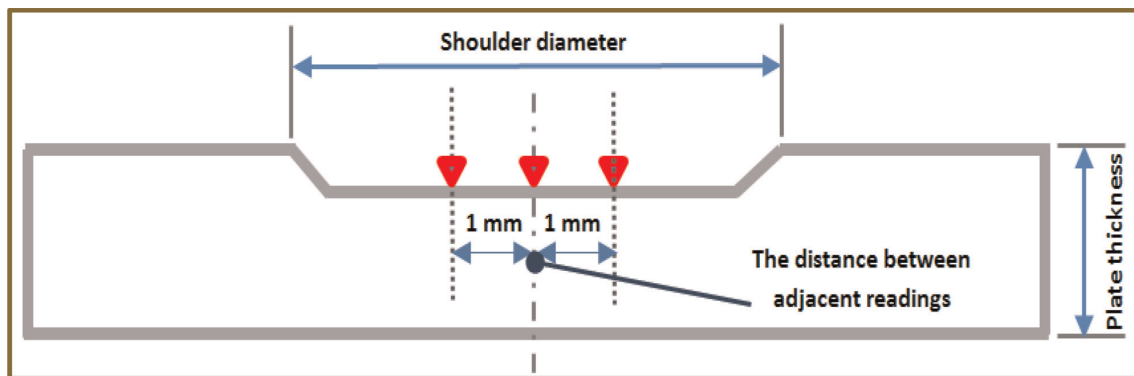

Figure 5.
Shows how to perform an accurate hardness reading.

size of m 1 and lubricating oil to produce a bright, scratch-free surface that resembles a mirror. In addition to water grinding, the sample may also be submerged in alcohol for a brief period of time, carried with specialized forceps, and then washed with running water after the polishing and polishing procedure. Finally, the samples undergo an exposition procedure (also known as etching) using Keller's reagent solution for 10–20 seconds. Following this, the samples are rinsed in water, their surfaces are cleaned with methanol alcohol, and they are dried by being placed in heated air. According to ASTM E3–01 [13], the microstructural investigation was performed on all samples at room temperature using the following materials: distilled water, concentrated hydrochloric acid (1.5 ml), concentrated nitric acid (2.5 ml), and concentrated fluoric acid (1.0 ml) (95 ml).

A magnification light microscope (X20) was used to prepare the samples for microscopic analysis, and the microstructure of the base metal and the other samples were discovered.

6. Friction stir processes (FSP)

The metallurgical and mechanical properties of the stir area change as a result of the heat produced by friction between the stir tool and the components to be welded

and the plastic deformation in the stir area during the stir process (FSP). A number of operational and engineering elements, such as the friction tool's rotating speed, the table's linear speed, the stir device's form and shape, the quantity of heat entering the stir region, and other considerations, have an impact on these changes.

6.1 The best model to use for the friction stir procedure

The sample of the optimum model, which achieves the best mechanical properties within the best suited parameters, was tested at the friction tool's rotating speed of 800 rpm and linear speed of 80 mm/min for one stage and a depth of 400 m, as indicated in **Table 5**. The average value of the modulus of elasticity in this case was (1.2%) compared to the base metal, and the greatest results were an increase in the average yield stress (16.9%) and maximum tensile stress (11.1%).

6.2 The impact of cutting depth on the friction stir process' microstructure

The original mineral's microstructure is made up of elongated grains with an average grain length of (187) m and a length-to-thickness ratio of (2.97), together with a heterogeneous distribution of precipitate particles as seen in **Figures 6** and 7.

The friction stir tool shoulder's spinning and pressing forces on the plate surface, along with the heat created by plastic deformation, cause a surface stirred layer (modified surface) to form beneath the tool shoulder to a depth of roughly a micrometer. The cutting depths (25, 50, 100, 150, 200, and 400 m) and stir layer were

No.	Travel speed *(mm/min)*	Tool rotation speed *(rpm)*	Specimen No.	Average Yield strength 0.2% offset y, *MPa* σ	Average Tensile strength $(S_{T,}MP)$	Elongation (%)	Modulus of Elasticity *(E, Gpa)*
			Base Metal	245	309	16	69.5
1	32	800	1	275	327	15	68.42
			2	271	333	16	69.61
2		1000	3	273	331	11	68.77
			4	279	335	14	71.87
3		1250	5	272	331	10	70.03
			6	274	336	12	71.07
4		1600	7	269	328	8	70.54
			8	272	335	9	71.27
5	63	800	9	271	333	9	60.91
			10	275	337	9	71.86
6		1000	11	280	337	10	63.45
			12	278	332	12	66.58
7		1250	13	268	335	10	66.71
			14	275	338	12	68.6
8		1600	15	272	329	12	63.06
			16	277	331	10	65.73

No.	Travel speed (mm/min)	Tool rotation speed (rpm)	Specimen No.	Average Yield strength 0.2% offset y, MPa σ	Average Tensile strength (S_T,MP)	Elongation (%)	Modulus of Elasticity (E, Gpa)
9	**80**	**800**	17	**285**	**338**	**12**	69.83
			18	288	**341**	**13**	70.89
10		**1000**	19	277	**328**	**13**	63.57
			20	272	325	13	65.33
11		1250	21	265	316	16	54.09
			22	271	337	13	71.95
12		1600	23	261	318	12	51.68
			24	263	322	12	68.42

Table 5.
The tests of the friction stir process of aluminum alloy (T6–6061) samples are compared for various rotational and linear speeds in order to select the optimal model for one stage and a depth of (400 m).

produced in two stages during the primary trials of the current study at an 800 rpm rotational speed and 80 mm/min travel speed, respectively. Both the first and second stages involve one pass each. From the chosen 800 rpm rotational speed with an 80 mm/min travel speed, **Figures 8–19** show all surfaces stirred layers created.

The reason for this is that the grains in the center of the friction area are smooth, equal in size along their axes, and smaller than the grains of the base metal. This is because the process of re-smoothing the crystalline sizes of the particles deposited in this area as a result of the plastic deformation caused by the high rotational movement of the friction tool and the occurrence of recrystallization as a result of the heat generated has occurred. As a result of the support's head (Shoulder) rubbing on the metal frame. Through a single analysis of the crystal structure of the friction process, as shown in the images of the microscopic structure of the alloy, Studying the crystal structure of the friction process for a single time allows us to observe that, while cutting from the surface of the original metal, there is
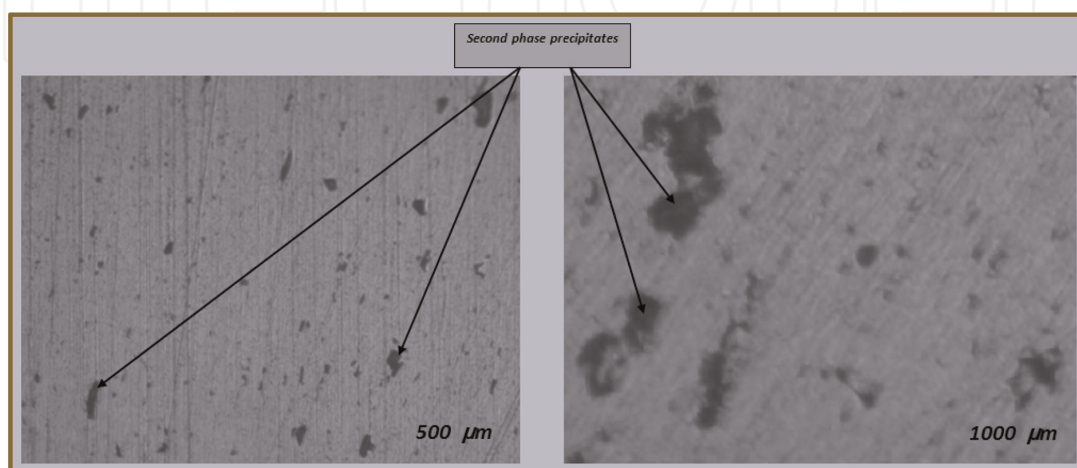

Figure 6.
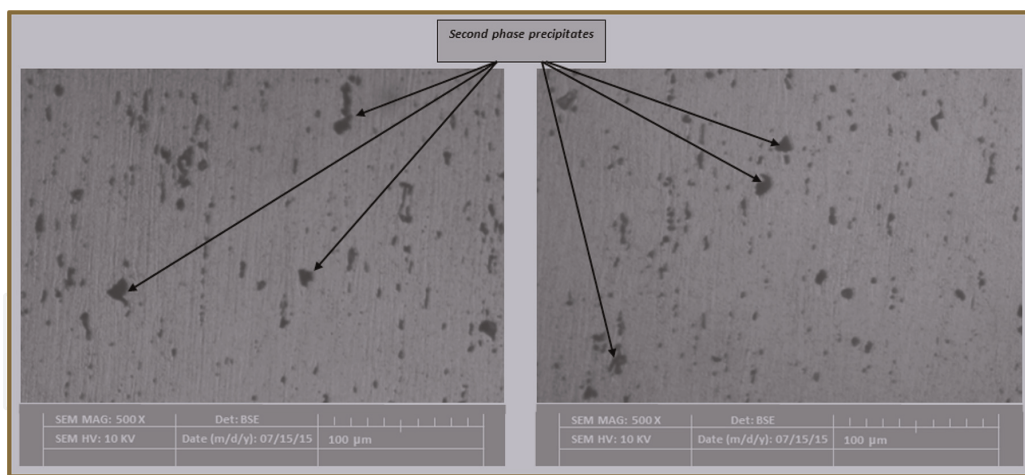*Show different magnifications of the basic mineral's microstructure (AA6061-T6).*

Figure 7.
Images captured by scanning electron microscopy of the aluminum alloy's base metal a backscattered electron micrograph and a secondary electron micrograph are also available.
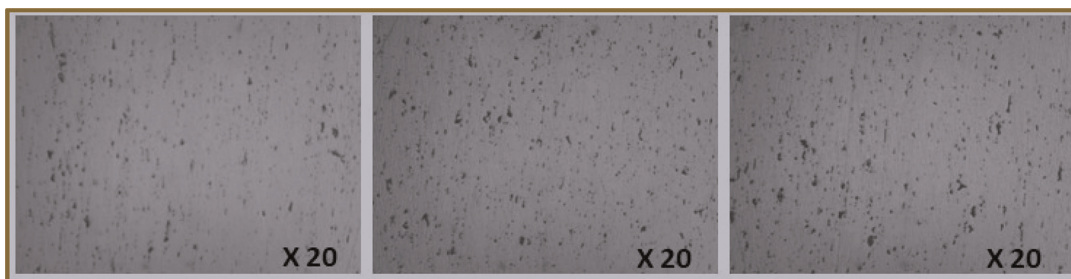

Figure 8.
Micrographs of the friction stir layer taken once at 0 μm depth, 800 rpm rotation speed, and 80 mm/min linear speed.

Figure 9.
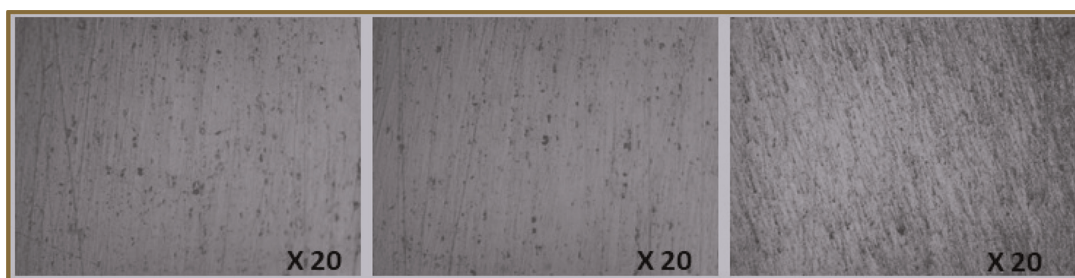*Micrographs of the friction stir layer cut once at a depth of 25 μm at an 800 rpm rotational speed and an 80 mm/ min linear speed.*

Figure 10.
Micrographs of the friction stir layer cut once at a depth of 50 μm at an 800 rpm rotational speed and an 80 mm/ min linear speed.
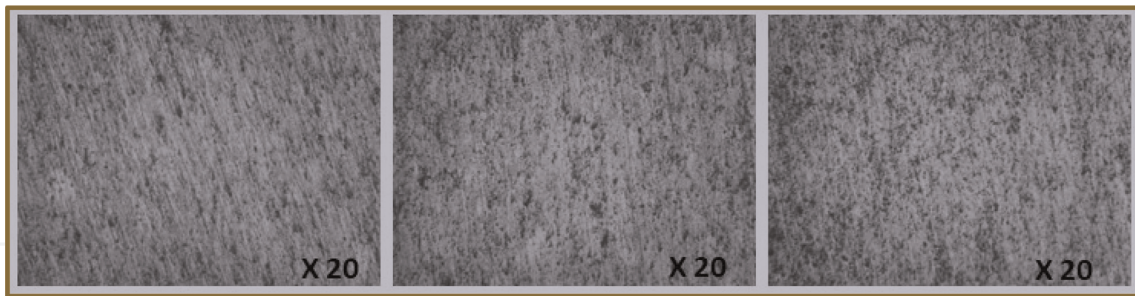
Figure 11.
Micrographs of the friction stir layer cut once at a depth of 100 μm at an 800 rpm rotational speed and an 80 mm/ min linear speed.
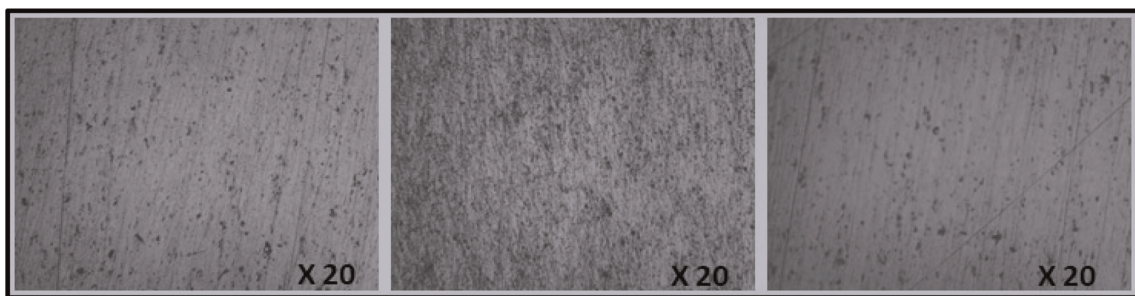

Figure 12.
Micrographs of the friction stir layer taken at a single 150 μm cutting depth, 800 rpm rotating speed, and 80 mm/ min linear speed.

Figure 13.
Micrographs of the friction stir layer taken at a single 200 μm cutting depth, 800 rpm rotating speed, and 80 mm/ min linear speed.

Figure 14.
Micrographs of the friction stir layer taken at a single 400 μm cutting depth, 800 rpm rotating speed, and 80 mm/ min linear speed.
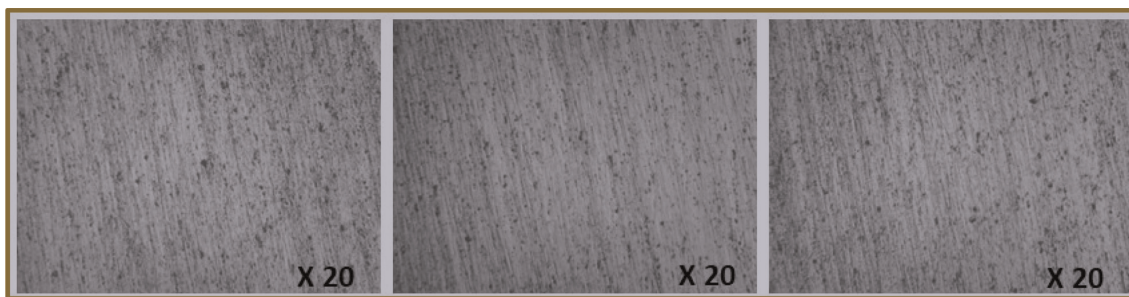
Figure 15.
Micrographs of the friction stir layer taken twice at a cutting depth of 25 μm and at 80 mm/min in linear motion and 800 rpm in rotation.
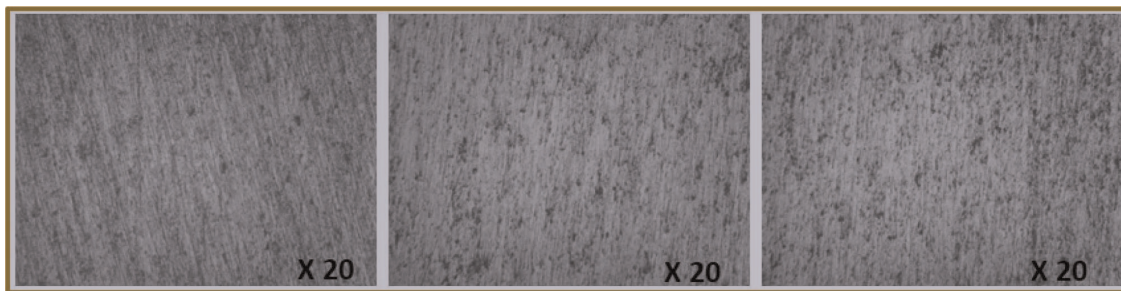

Figure 16.
Micrographs of the friction stir layer taken twice at a cutting depth of 50 μm and at 80 mm/min in linear motion and 800 rpm in rotation.

Figure 17.
Micrographs of the friction stir layer taken twice at a cutting depth of 100 μm and at 80 mm/min in linear motion and 800 rpm in rotation.
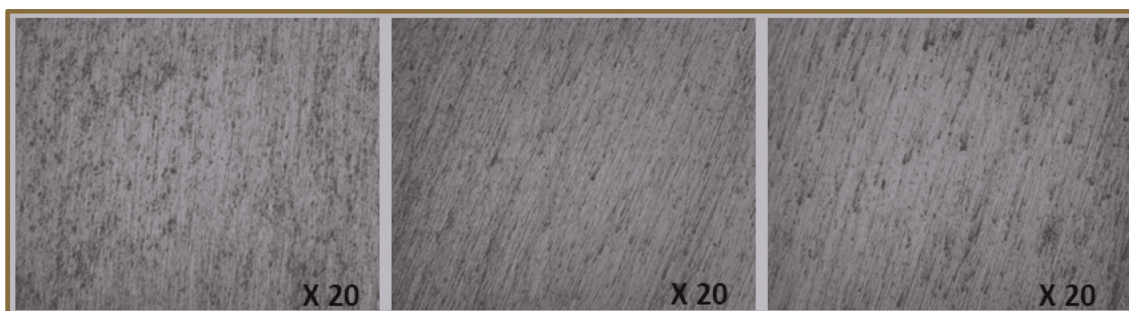

Figure 18.
Micrographs of the friction stir layer taken twice at a cutting depth of 200 μm and at 80 mm/min in linear motion and 800 rpm in rotation.
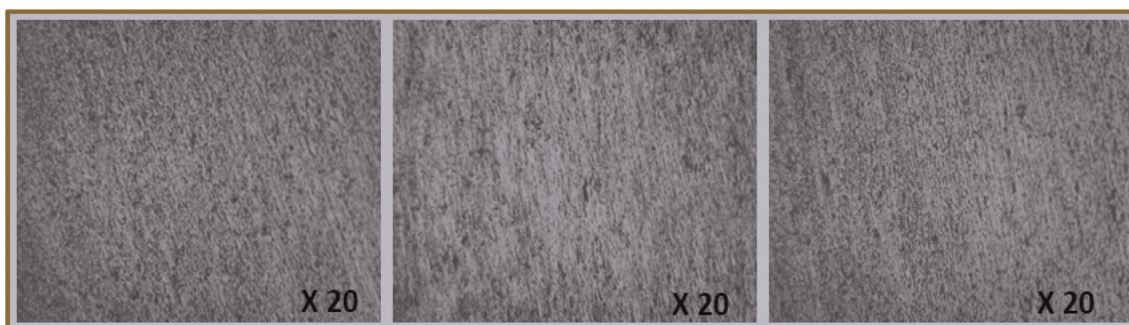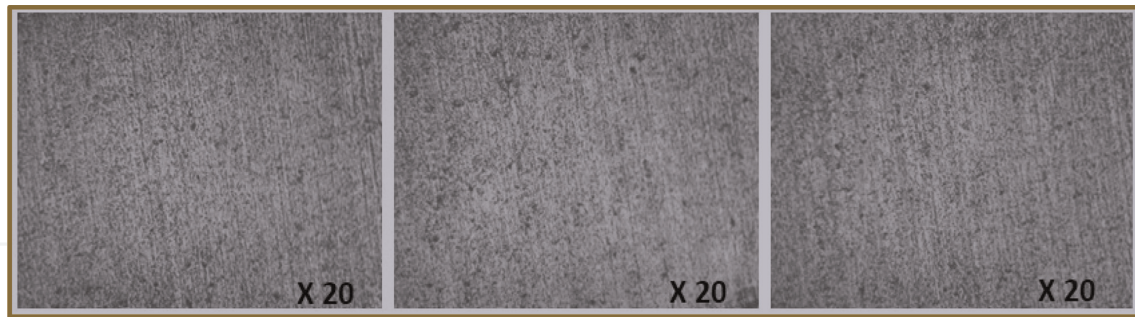
Figure 19.
Micrographs of the friction stir layer taken twice at a cutting depth of 400 μm and at 80 mm/min in linear motion and 800 rpm in rotation.

a percentage reduction in the size of the geometric flaws of the metal surface as follows:

When the depth of the cut was (25 m), the percentage of the size of the defects decreased (3.03% size), at (50 m, the percentage of decrease was approximately (3.32% size), at (100 m), the decrease was clearly greater, reaching (21.61% size), at (150 m), it was (30.42% size), at (200 m), it was (38.32%), and the highest decrease was recorded when the depth of the cut was (400 m).

The size of the fault grains in the metal surface decreased in comparison to the surface of the original metal in the following ways: The depth of cut at (25 m) was (4% size), the depth at (50 m) was (6% size), the depth at (100 m) was (10% size), the depth at (150 m) was (35% size), the depth at (200 m) was (38% size), and the depth at (400 m) had the largest percentage of grain size decrease, which amounted to (400% size).

Observe from the crystal structure and analysis that the geometric flaws have smaller grains and that the size of these grains reduces as the depth of cut increases. Furthermore, there is a greater proportion of shrinking and smallness in the friction process over two times than there is in the friction process over one time.

6.3 The impact of cutting depth on the friction stir process' mechanical characteristics

For the friction stir process of aluminum alloy samples (T6–6061), the necessary mechanical examination tests (hardness examination, tensile test, finding the value of the elastic modulus, and finding the value of yield strength) are carried out at a rotational speed (800 rpm) and a linear speed (mm/min80) for one and two times as well as for different depths of the process. Surface stir caused by friction. The outcomes are displayed in the **Tables 6** and 7.

The frictional mixing process's cutting depth and the hardness value are related in **Figure 20**. The figure clearly illustrates the relationship between the cutting depth and the hardness value in the case of the friction mixing process for two times, and it also indicates that this rise in hardness value remains considerable up to a depth of (300 mm). As the cutting depth is increased to stroke (300 mm), the hardness value increases dramatically, however this growth is drastically decreased. Additionally, a comparison between the single and double frictional mixing cases, where the hardness value rises as the cutting depth increases In addition, the amount of frictional mixing that occurs during a double frictional mixing process is greater than it is during a

Cutting depth μm	Specimen No.	Average Yield strength 0.2% offset y σ MPa	Average Tensile strength S_T MPa	Modulus of Elasticity E GPa	Elongation %	Hardness HV Kg/mm²	Average Hardness HV Kg/mm²
Base Metal		245	309	69.5	16	101.5	101.5
0	36	247	311	70	14.4	100.8	101.6
	37	259	310	71	14.6	102.4	
	38	260	313	67	15.1	101.7	
25	39	267	315	69	12.2	101.3	102.2
	40	263	318	67	9.7	101.1	
	41	272	316	69	8.0	104.2	
50	42	272	322	67	10.6	105.5	103.5
	43	270	325	68	11.5	101.6	
	44	269	322	69	15.1	103.4	
100	45	279	324	68	11.0	104.5	104.1
	46	280	327	69	11.9	103.1	
	47	277	331	69	12.9	104.7	
150	48	283	331	66	15.0	100.6	104.3
	49	282	326	70	10.8	108.1	
	50	278	336	69	10.2	104.2	
200	51	281	328	69	12.2	110.7	108.1
	52	286	339	70	12.6	108.1	
	53	282	334	67	17.4	105.6	
300	54	281	336	71	10.2	112.7	110.7
	55	285	330	67	9.1	111.8	
	56	288	341	71	8.7	107.6	
400	57	289	343	72	14.0	112.1	110.9
	58	282	333	69	13.1	108.8	
	59	284	339	70	13.6	111.7	

Table 6.
Compares the results of the friction stir experiments conducted on samples of aluminum alloy (T6–6061) at two different speeds: 800 rpm for rotation and 80 mm/min for linear motion, for one stage of the surface.

Cutting depth μm	Specimen No.	Yield strength 0.2% offset y σ MPa	Tensile strength S_T MPa	Modulus of Elasticity E GPa	Elong. %	Hardness HV Kg/mm²	Average Hardness HV Kg/mm²
Base Metal		245	309	68	16	101.5	101.5
50	60	275	324	62.33	11.9	105.9	103.5
	61	273	322	58	11.3	103.7	
	62	276	323	44	8.7	100.8	

Cutting depth μm	Specimen No.	Yield strength 0.2% offset y σ MPa	Tensile strength S_T MPa	Modulus of Elasticity E GPa	Elong. %	Hardness HV Kg/mm^2	Average Hardness HV Kg/mm^2
100	63	284	328	46.36	15.1	104.6	106.1
	64	279	330	44.77	13.8	109.6	
	65	285	331	49.78	13.2	104.1	
150	66	284	339	53.75	14.9	112.6	113.4
	67	287	340	59.42	14.4	115.6	
	68	284	337	54.77	15.6	112.1	
200	69	289	340	58.75	14.6	119.1	117.2
	70	284	342	58.64	14.8	115.2	
	71	286	340	59.33	12.2	117.3	
300	72	288	342	54.35	12.8	122.6	123.3
	73	292	344	52.15	14.6	124.1	
	74	289	340	53.47	13.7	123.1	
400	75	290	345	53.35	11.9	125.1	124.2
	76	288	344	50.5	11.3	120.5	
	77	295	345	52.48	8.7	127.1	

Table 7.
Compares the results of tests on the friction stir process for samples of aluminum alloy (T6–6061) at two different speeds: 800 rpm for rotation and 80 mm/min for linear motion.
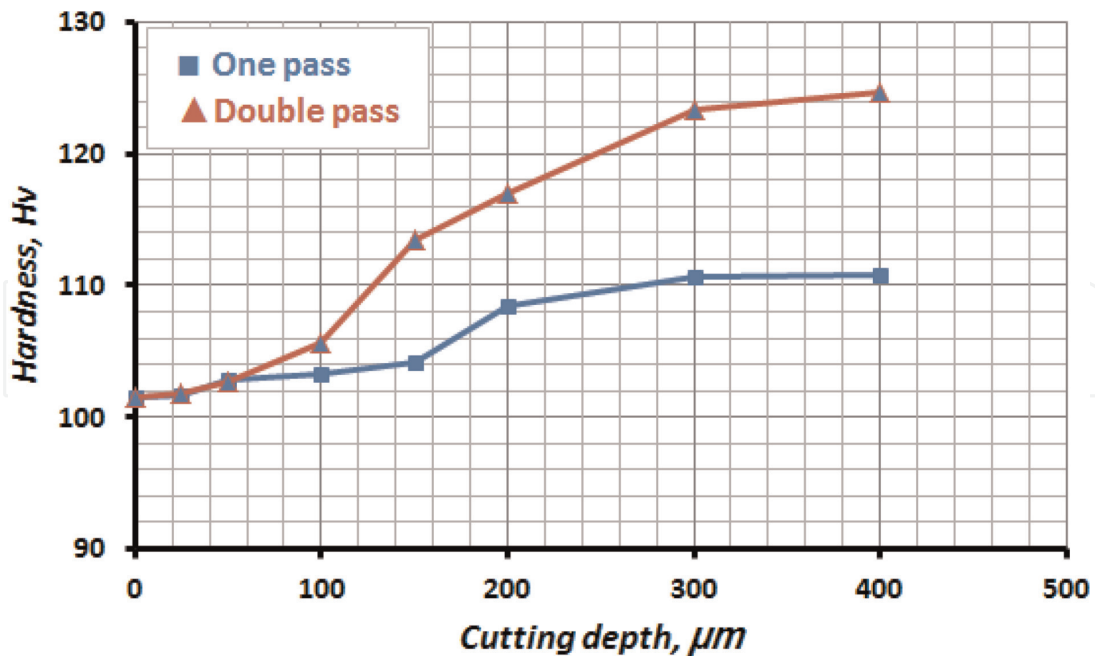

Figure 20.
Shows the connection between the hardness value and the frictional mixing process' cutting depth. Comparison of the mixing processes used once and twice.

single frictional mixing process. This is because the homogeneity of the crystals is greater, and the high temperature of the double frictional mixing process results in a reduction in engineering flaws and impurities.
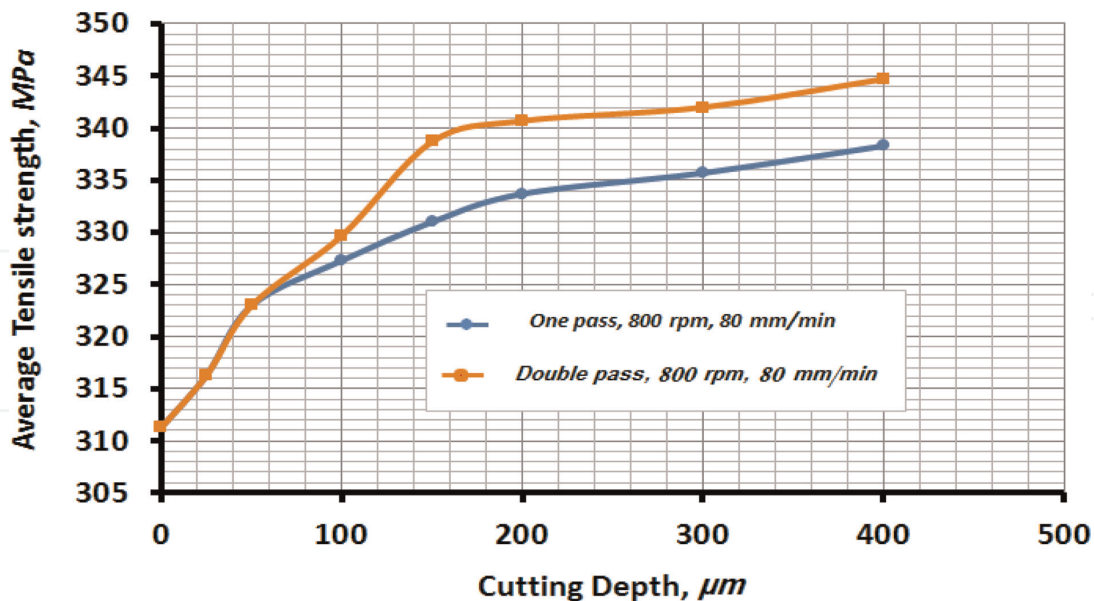
Figure 21.
Shows the relationship between the value of the tensile stress rate and the cutting depth of the friction mixing process. Comparison of the mixing processes used once and twice.

The maximum tensile stress rate increases with the increase in cutting depth, as shown in **Figure 21**, which contrasts the cases of the single and double friction mixing processes. Additionally, the double frictional mixing procedure is (2%) more efficient than the single frictional mixing technique.

7. Conclusions

The following conclusions can be reached after doing the study, reviewing, and discussing the findings:

1. The results of the examination and analysis show that the hardness increases with an increase in the cutting depth in the friction mixing processes; for one stage of frictional mixing, it increased by 9.3%, and for two stages, it increased by 22.4% compared to the base metal and at a depth of (400 m), and the increase is greater in the mixing process. With a rate of 13.1%, frictional mixing occurs twice from frictional mixing occurs once.

2. It is also clear from the microscopic structure of the samples that were subjected to the friction mixing processes that increasing the friction mixing process' cutting depth increased the homogeneity of the crystals and significantly reduced the number and size of engineering defects and impurities. Additionally, the reduction is greater when combining twice.

3. For one stage of the frictional mixing process, the yield strength increases by 18%, the tensile strength by 9.5%, and for two stages of the frictional mixing process, the yield strength increases by 20.4% and the tensile strength by 11.5%.

4. One stage of the friction mixing process improves the rate of hardness by 8.3% compared to the base metal, and two stages of the friction mixing process increase the rate of hardness by 18% compared to the base metal.

5. As the welding tool's rotating speed is increased, the bending resistance reduces while the welding table's linear speed increases. Using a friction mixing welding tool with a square indentation bump as opposed to one with a conical bump improves the bending resistance (cone).

Author details

Emad Toma Bane Karash* and Mohammad Takey Elias Kassim
Department of Mechanical Technologies, Mosul Technical Institute, Northern Technical University, Mosul, Iraq

*Address all correspondence to: emadbane2007@ntu.edu.iq

IntechOpen

References

[1] Zakharov VV. Aluminum alloys: Some problems of the use of aluminum – Lithium alloys. Metal Science and Heat Treatment. 2003;**45**(1–2):49-54

[2] Akula DR. Characterization of Mechanical Properties and Study of Microstructure of Friction Stir Welded Joints Fabricated from Similar and Dissimilar Alloy of Aluminum. Columbia: Degree Master of Science, University of Missouri; 2007

[3] Odeshi AG, Adesola AO, Badmos AY. Failure of AA 6061 and 2099 aluminum alloys under dynamic shock loading. Engineering Failure Analysis. 2013;**35**: 302-314. DOI: 10.1016/j. engfailanal.2013.02.015

[4] Periyasamy YK, Perumal AV, Periyasamy BK. Optimization of process parameters on friction stir welding of AA7075-T651 and AA6061 joint using response surface methodology. Materials Research Express. 2019;**6**: 96558-96584

[5] Husain Mehdi RS. Mishra, Efect of friction stir processing on microstructure and mechanical properties of TIG welded joint of AA6061 and AA7075. Mater. Metallography Microstructure and Analysis. 2020;**9**(3):1-10. DOI: 10.1007/s13632-020-00640-7

[6] Refaai MRA, Reddy RM, Radha A, Christopher D. The influence of process parameters on the mechanical properties of friction stir-welded dissimilar Aluminium alloys AA2219 and AA7068. Advances in Materials Science and Engineering. 2022;**2022**, Article ID 3104199, 9 pages:1-9. DOI: 10.1155/2022/ 3104199

[7] Murali S, Chockalingam A, Suresh Kumar S, Remanan M. Production, characterization and friction stir processing of AA6063-T6/Al3Tip in-situ composites. International Journal of Mechanical and Production Engineering. 2018;**6**:399-406 View at: Google Scholar

[8] Manikandan R, Elatharasan G. Effect of process parameters on microstructural and mechanical properties of friction stir welded dissimilar aluminium alloys AA 6061 and AA 7075. International Journal of Rapid Manufacturing. 2020;**9**(1):1-15 View at: Publisher Site | Google Scholar

[9] Pasha A. Fabrication of surface metal matrix composite of AA7075 using friction stir processing. International Journal of Scientific Research in Science and Technology. 2022;**9**(3): 551-555 https://doi.org/10.32628/ IJSRST2293108

[10] Kumar K, Gulati P, Gupta A, Shukla DK. A review of friction stir processing of Aluminiumalloys using different types of reinforcements. International Journal of Mechanical Engineering and Technology. 2017;**8**(7): 1638-1651

[11] Salman JM. A comparative study an additives of nickel, cobalt, tin affecting the micros tructures and mechanical properties of Al-Zn-Mg-Cu alloys. Journal of Babylon University/ Engineering Sciences. 2014;**76**(3)218-235. DOI: 10.13140/RG.2.2.12531.43043

[12] Murali VV, Satyanarayana K. Microstructure and mechanical properties of multipass friction stir processed aluminum silicon carbide metal matrix. International Journal of Scientific Engineering and Technology (ISSN: 2277-1581) Volume No. 4 Issue No. 2015;**2**:88-90

[13] Karthikeyan L, Senthilkumar VS, Balasubramanian V, Natarajan S. Mechanical property and microstructural changes during friction stir processing of cast aluminum 2285 alloy. Materials and Design. 2008;**30**: 2237-2242

[14] El-Danaf EA, El-Rayes MM, Soliman MS. Friction stir processing: An effective technique to refine grain structure and enhance ductility. Materials and Design. 2010;**31**:1231-1236

[15] ASTM E 384 – 99, Standard Test Method for Micro indentation Hardness of Materials. Conshohocken, PA, United States: ASTM; 2000. Standard_Test_Me thod_for_Microindentatio.pdf

[16] ASTM E8M – 04. Standard Test Methods for Tension Testing of Metallic Materials [Metric]. West Conshohocken, PA, United States: An American National Standard American Association State Highway and Transportation Officials Standard AASHTO No.: T68, ASTM International; 2004

[17] ASTM E 290 – 9. Standard Test Method for Bend Testing of Material for Ductility. USA, 2009. www.xycxie.com (chem17.com)

[18] ASTM E 23. Sub – Size Charp y, V Notched Specimens. Standard Test Methods for Notched Bar Impact Testing of Metallic Materials. USA, 2005

[19] Wang X, Lados D. Understanding the material flow mechanisms microstructure evolution defect formation relationships and effects on mechanical properties in friction stir welding of dissimilar aluminum alloys. Metallurgical and Materials Transactions A Published by ASM International. 2022; **54**:5. DOI: 10.1007/s11661-022-06921-w

[20] ASTM E23-18. Notched Bar Impact Testing of Metallic Materials1|PDF| Fracture|Temperature (scribd.com)